G.Ghigo, A.Chodoni, R.Gerbaldo, L.Gozzelino, F.Laviano, E.Mezzetti, B.Minetti

INFM U.d.R.To-Politecnico; INFN Sez.Torino; Politecnico di Torino, Torino, Italy

G. Rotoli and C. De Leo

Università dell'Aquila, INFM – U.d.R. L'Aquila, L'Aquila, Italy

C. Camerlingo

Istituto di Cibernetica del Consiglio Nazionale delle Ricerche, Arco Felice, Italy

C. Giannini

Pa.S.T.I.S.–C.N.R.S.M., Brindisi, Italy

Networks of nanosized Josephson junctions as reference structures for macroscopic transport properties in YBCO films

PART I

Fabrication process

The $YBa_2Cu_3O_{7-\delta}$ superconducting films were fabricated in situ by dc sputtering from inverted cylindrical magnetron on $SrTiO_3$ (100) oriented substrates.

Two kind of films were produced:

standard cooling process
→ fully oxygenated film (F)
slightly modified cooling process
→ oxygen deficient film with defected GBs (D).

Susceptibility transition

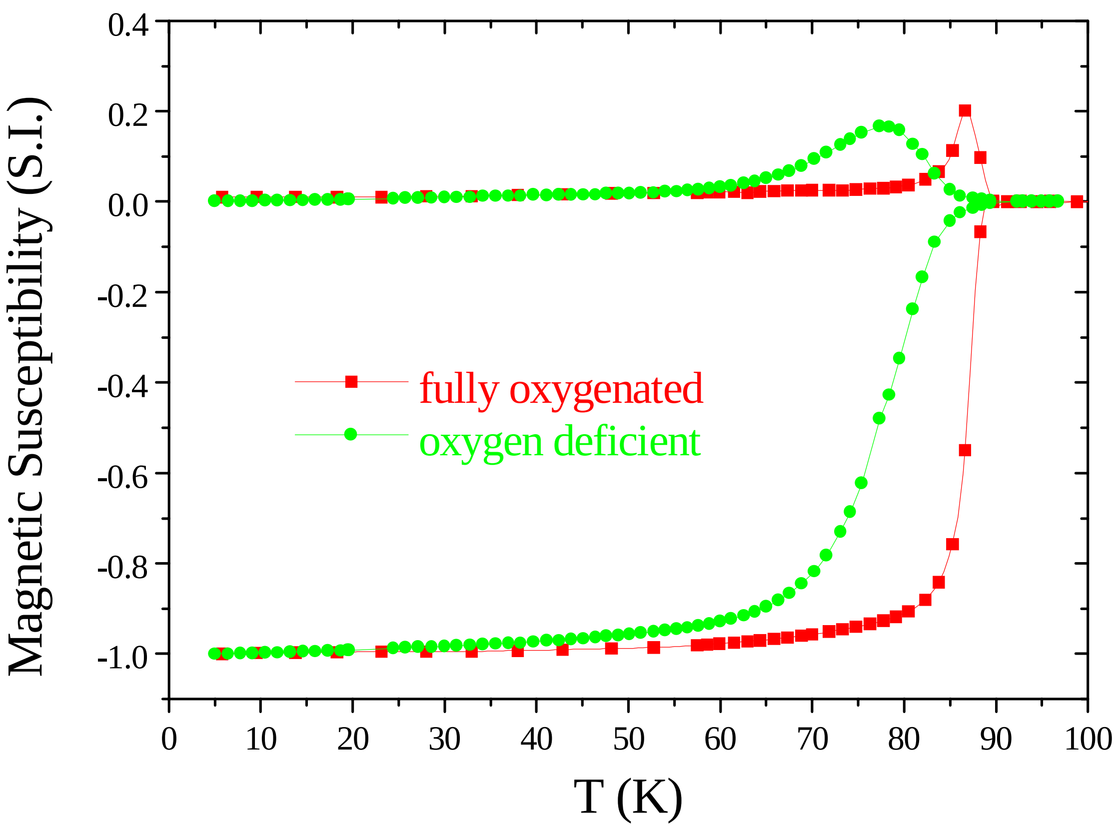

Raman analysis

Position of the line $\nu_H \Rightarrow$ oxygen content $\Rightarrow$

films (D): $\delta = 0.34$
films (F): $\delta = 0.02$ *in the $YBa_2Cu_3O_{7-\delta}$ formula*

The large Raman line appearing in the spectra of samples (D) at 230 cm^{-1} and the broad band at 580 cm^{-1} can be attributed to vibration modes associated with oxygen defects.

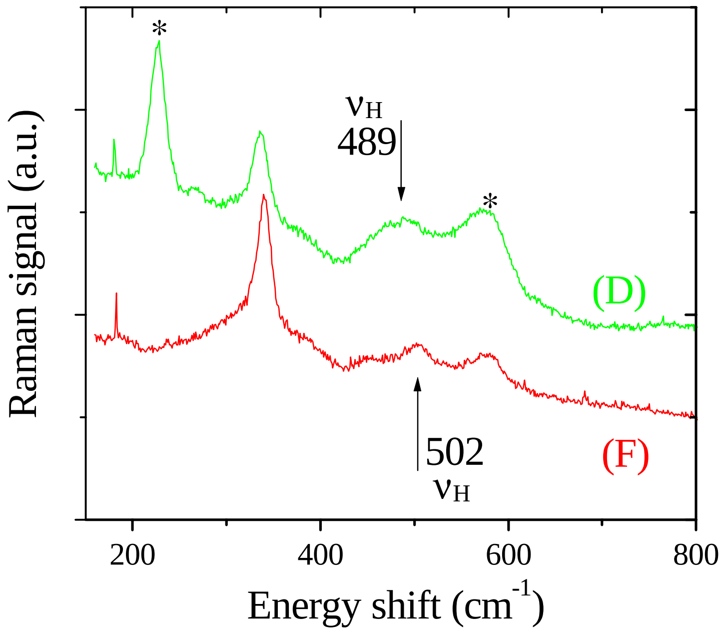

The samples (D) exhibit disorder in the oxygen sublattice, with broken CuO chains and probably the setup of out of phase oxygen microdomains

X-ray diffraction

These features do not affect the crystalline properties of the films, strong crystal orientation in the θ–2θ X-ray diffractogram, with c-axis directed normal to the surface plane

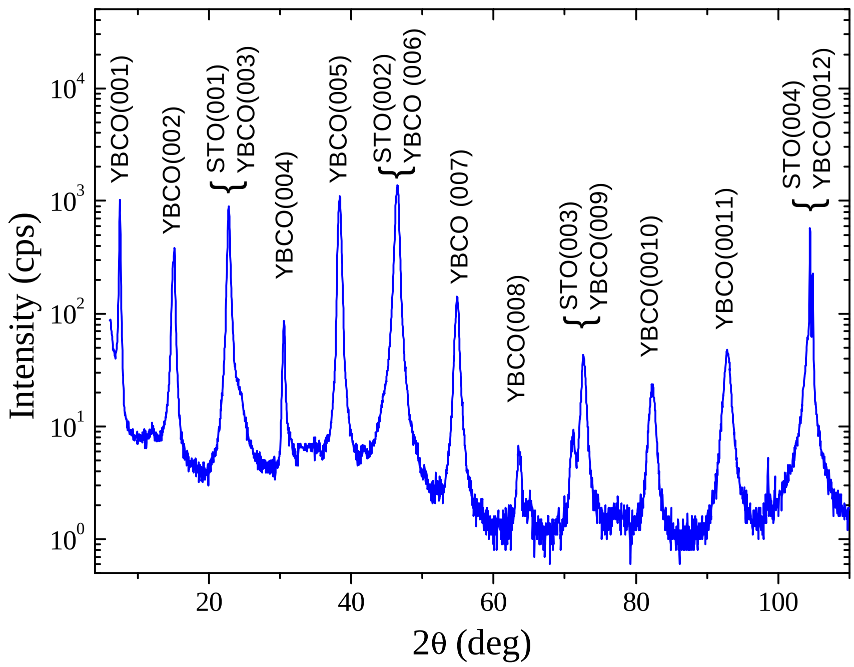

Critical current density evaluation

- *First harmonic susceptibility data were analyzed in the framework of the Clem and Sanchez model for the case of a thin sample in a transverse field*

  [J.R.Clem and A.Sanchez, Phys. Rev. B ***50****, 9355 (1994)]*

- *We extracted the values of the critical current density by numerically inverting the relation*

$$\chi' = \frac{2\chi_0}{\pi}\int_0^{\pi}(1-\cos\vartheta)\, S[(x/2)(1-\cos\vartheta)]\cos\vartheta\, d\vartheta$$

$$S(x) = \frac{1}{2x}\left[\cos^{-1}\left[\frac{1}{\cosh x}\right] + \frac{\sinh x}{\cosh^2 x}\right] \quad ; \quad x = h_0/H_d = 2h_0/(J_c t)$$

where h_0 *is the amplitude of the ac field and* t *is the sample thickness.*

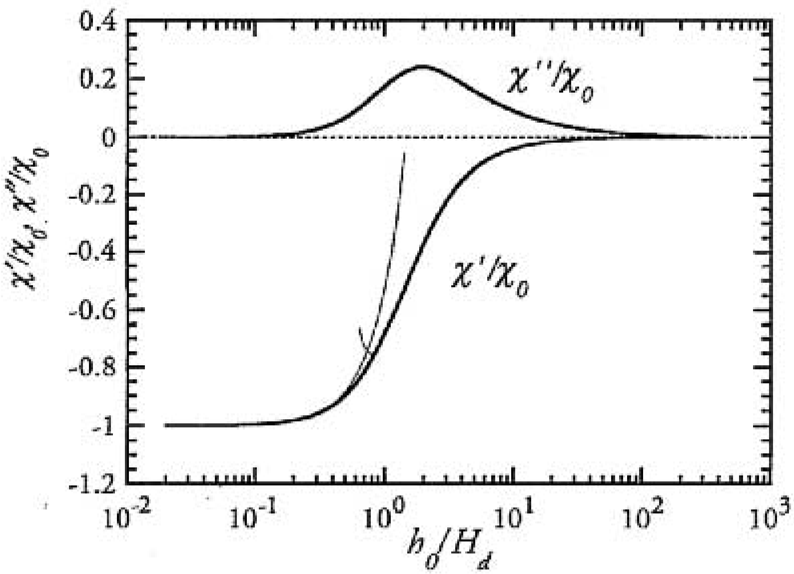

- *The application of a dc field does not modify this expression as long as the critical current is weakly field-dependent.*

MODEL - introduction

- *A satisfactory model of flux confinement and current carrying mechanisms for interfaces in HTS films is not yet available to date, due to two reasons:*
  1) *the interaction concerns a huge number of confining elements (strongly interacting with each other and, in principle, exhibiting unknown relevant long range interactions)*
  2) *the distribution and size of the potential wells contains a certain degree of disorder and is unknown to a large extent.*

- *Grain boundaries in good quality YBCO films are high-J_c junctions, playing the role of "hidden" weak links*

[A.Gurevich, Phys. Rev. B 50 (1994) 13563]

simple model based on the existence of a JJ network

↓

one dimensional array of parallel, decoupled uniform short Josephson junctions

+ statistical distribution of junction lengths

+ field dependent magnetic thickness

FITTING PROCEDURE

EXAMPLE

$$J_c(B) = J_c(0)\frac{1}{\Gamma(\nu) q\sqrt{B}}\int_0^\infty x^{\nu-2}e^{-x}\left|\sin(q\sqrt{B}x)\right|dx$$

$$q = \pi\frac{\zeta < L >}{\nu\sqrt{\phi_0}} \qquad \nu = \left(\frac{< L >}{\sigma}\right)^2$$

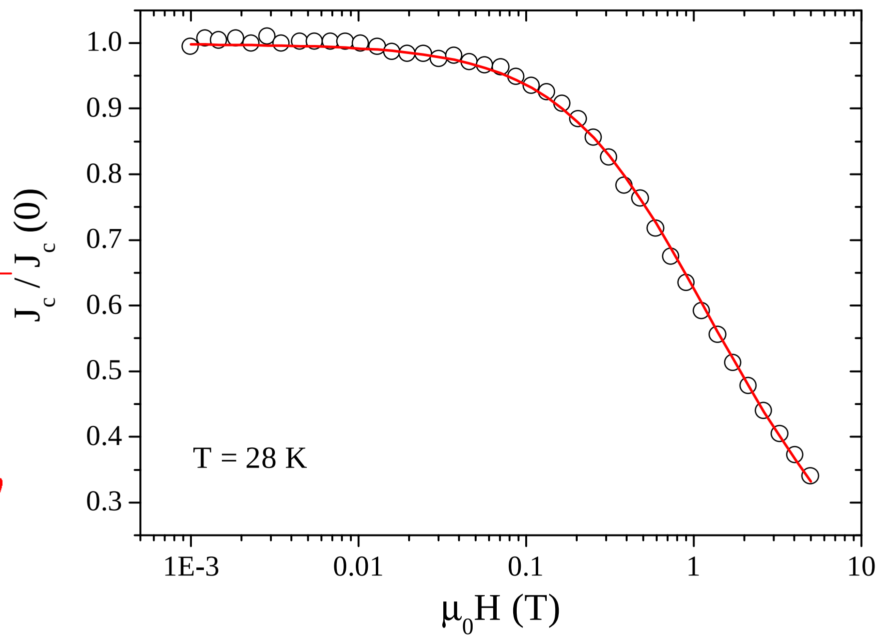

<L>ζ = 24 nm
<L>/σ = 1.4

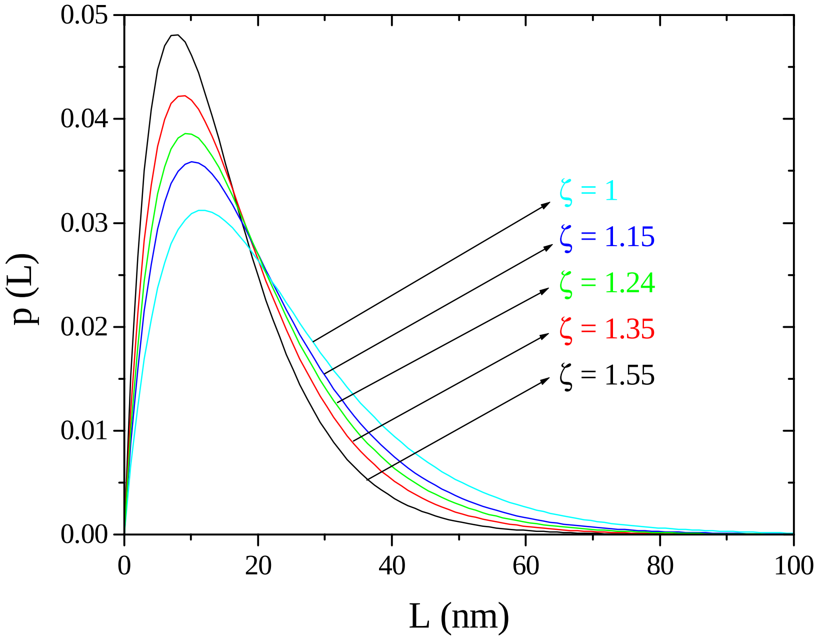

- *Critical current density vs. applied magnetic field as deduced from the susceptibility measurement. J_c experimental data (symbols) have been fitted (solid line) by means of the model described above.*
- *The fitting procedure results in the determination of the two physical quantities <L>ζ and <L>/σ.*
- *The corresponding junction-length distributions are reported in the lower panel for different ζ□ values.*
- *The fitting procedure is successful with both oxygen-deficient, fully-oxygenated and irradiated films.*

IN ORDER TO OBTAIN ALL THE PHYSICAL PARAMETERS INTO PLAY, WE NEED AN INDEPENDENT DETERMINATION OF THE JUNCTION LENGTH DISTRIBUTION p(L)

COMPARISON BETWEEN THE TRANSPORT PROPERTIES AND THE STRUCTURAL PROPERTIES OF THE HOST MATERIALS ON A NANOMETER SCALE	*THE JUNCTION LENGTH DISTRIBUTION p(L) AND THE GRAIN-SIZE DISTRIBUTION p(D) ARE VERY SIMILAR AND DISPLAY THE SAME NAMETRIC SCALES*

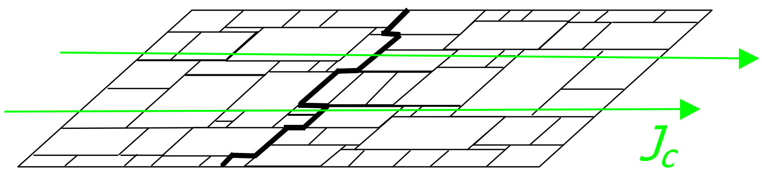

p(L) ⟺ p(D)

On the basis of this correspondence, we used the p(D) distribution to obtain new fits of the experimental Jc vs. B curves. *In this second analysis the only free parameter left is ζ*

DETERMINATION OF THE ***GRAIN SIZE***

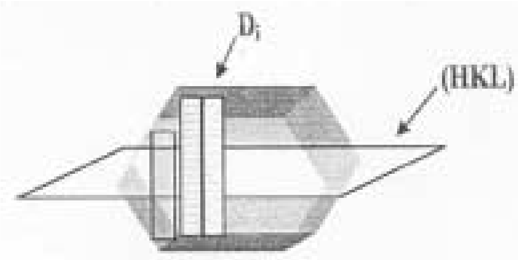

The model considers the diffracting object as composed by columns of slightly different size D, each column lying perpendicular to the (HKL) diffraction plane.

Each column consists of stacking of unit cells and contributes incoherently with one another to the total scattering intensity. According to the column-like model, the diffraction line can be written as the weighted sum of discrete elements:

$$I(s - s_0) = \sum_{i,j} \Phi(s - s_0, D_i, \varepsilon_j)\, W(D_i, \varepsilon_j)$$

where $\varepsilon_j = \Delta d_j / d_0$ is the mean lattice distortion over the j^{th} column and D_i is the size of the i^{th} column.

A Montecarlo procedure is performed to find out the grain size distribution $W(D_i, \varepsilon_j)$ that best approximates, in a least square sense, the measured rocking curve.

[P.E. Di Nunzio, S. Martelli, R. Ricci Bitti, J. Appl. Cryst. 28 (1995) 146]

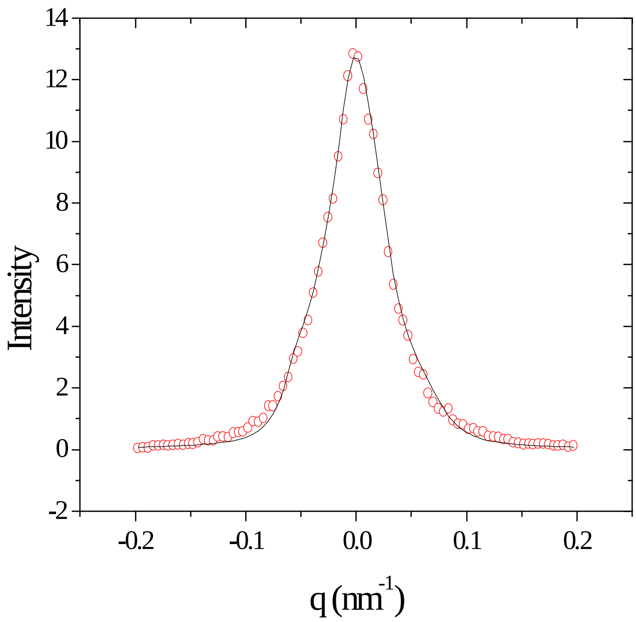

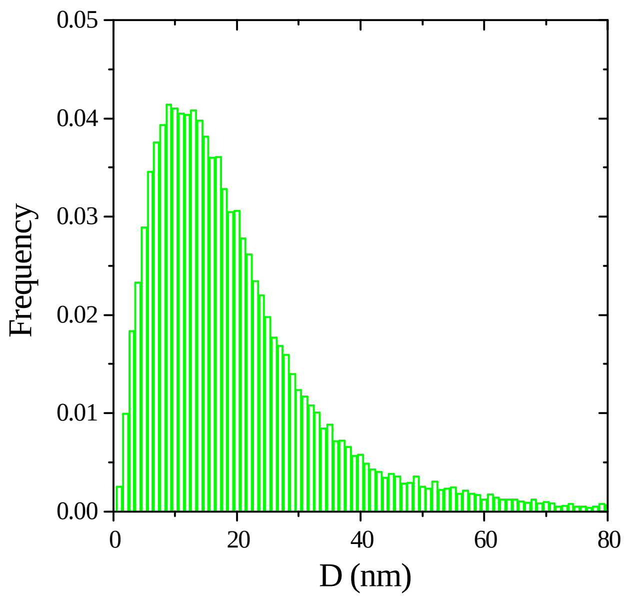

DETERMINATION OF ζ and J_c-B ***SCALING***

only 1 fitting parameter: ζ

from X-ray analysis

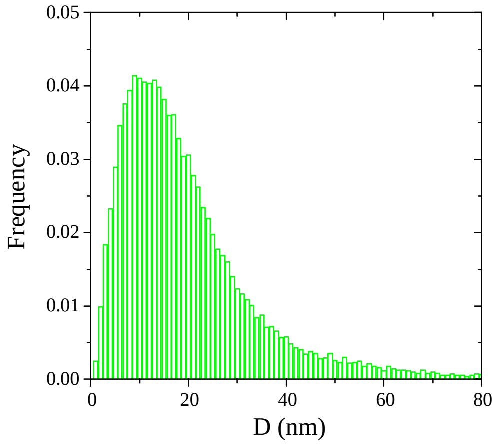

p(D) = p(L)

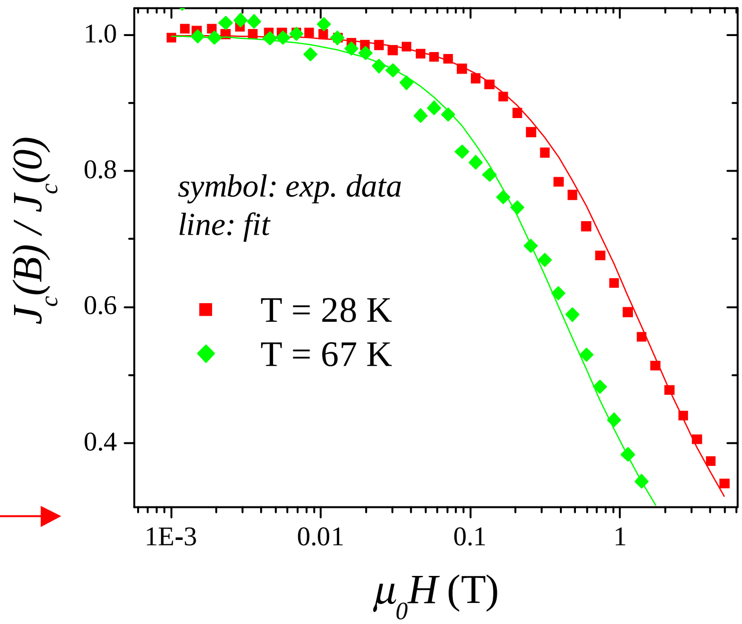

T (K)	*ζ*
28	*1.24*
36	*1.27*
47	*1.28*
55	*1.77*
67	*2.19*

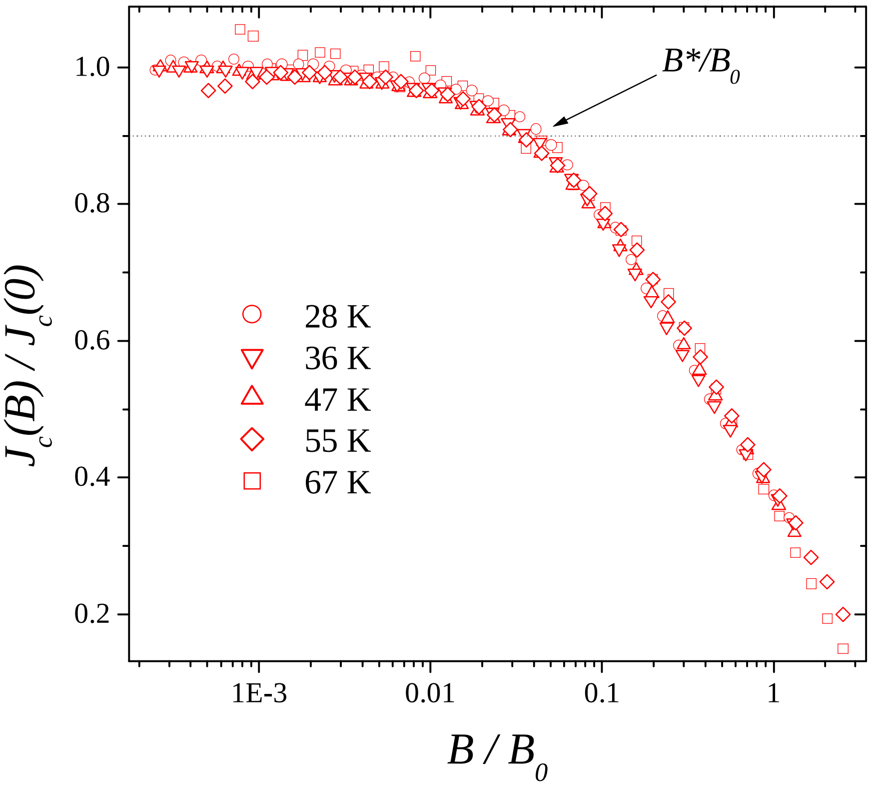

$$J_c(B) = \int_0^\infty dL\, p(L)\, J_c(0) \left| \frac{\sin(\pi\sqrt{B/B_0})}{\pi\sqrt{B/B_0}} \right|$$

$B_0 = \Phi_0 / \zeta^2 L^2 \Longrightarrow B_0 = \Phi_0 / \zeta^2 \langle L \rangle^2$

PART I - CONCLUSIONS

- *We have found a striking correlation between nano-sized structural patterns in YBCO sputtered films and their macroscopic transport current*

- *A model based on the presence of a network of Josephson junctions with statistically distributed junction-lengths and field-dependent magnetic thickness accounts for the measured J_c vs. B behavior*

- *The comparison between the macroscopic J_c measurement and the structural analysis on a nanometric scale enables us to determine the properties of the Josephson junctions involved in the transoprt mechanism and to find out a scaling law for J_c in the (B,T) plane*

References

E. Mezzetti et al., Physical Review B **60** (1999) 7623

G. Ghigo et al., Superconductor Science and Technology **12** (1999) 1059

G. Ghigo et al., Philos. Mag. B, **80** (2000) 865

E. Mezzetti et al., Physica C, **332** (2000) 115

C. Camerlingo et al., Physica C, **332** (2000) 93

G. Ghigo et al., Physica C, in press (2000)

Part II - Introduction

In this part we make an analysis of the JJ network as a discrete set of parallel junctions (1D Josephson array), in quasi-static conditions. One dimensional arrays was suggested very early in the study of HTC.

Superconductors [1], though their applications was limited to phenomenological considerations by complex nature of phenomena occurring in HTC bulk materials. Only recently considerations on the physics of HTC YBCO films make possible modeling the film transport properties as flow of supercurrents through links between granular structure of the film [2]. The coupling between the junctions of the array is introduced via standard fluxoid quantization rule and self-inductance of superconducting path between junctions of the network. In this model the coupling is represented by a suitable value of the parameter:

$$\beta = \frac{2\pi I_0(0)L}{\Phi_0}$$

Single junctions of the network are modeled as RSJ elements (at this moment all perfectly equal without spread in the critical currents or electrical

parameters with an intermediate damping corresponding to β_C).
Equations describing the array can be written as DSG (Discrete Sine-Gordon) equation in the following form [3,4]:

$$\vec{\varphi}_{tt} + \alpha \vec{\varphi}_t = \mathbf{M}\vec{\varphi} + \tilde{\mathbf{A}}\vec{f} + \vec{\gamma}$$

here $\vec{\varphi}$ and $\vec{f}$ are respectively the phase vector representing the phase in each junction and the frustation vector, $\tilde{\mathbf{A}}$ is the matrix relating frustation to phases, $\mathbf{M}$ is the coupling matrix which is proportional to $1/\beta_L$ and contains in general both self-inductance and mutual inductance terms (here we consider only next neighbor mutual inductances), $\alpha = 1/\sqrt{\beta_C}$ is the damping parameter, finally $\vec{\gamma}$ is the induced bias current vector (in this model representing the AC magnetization current generated in the sample). In order to reproduce the transport current mechanism used in the experiments magnetic field was introduced only at one extreme (active end) of the array representing the physical edge in which the field penetrate in the film progressively advancing toward the full penetration toward the center of the sample, represented by the other extreme of the array (passive end).

An illustration of the dynamics of JJ array is shown in Fig.1a: where we report the normalized current as function of Rotation Number, i.e. the number of flux quanta entering the array, for three values of active end normalized magnetic field as shown in the legend. The critical state is reached at the end of each curve. The parameters of the array are the following: β_L =225, N=40, α=1. In a typical simulation current bias current is increased starting from zero in a given magnetic field until array becomes critical and a finite voltage apppears at its ends. Before critical current is reached due to strongly discrete nature of system several avalanches of (Josephson) vortex (fluxons), corresponding in this model to a 2π wrap in the phases, penetrate in the array from the active end This process continue until the array is uncapable to accomodate other fluxons because it will be completely penetrated by the field and no room is found for other fluxons. At this values of bias current critical state sets on. For lower current values the dynamical mechanism of penetration of the field in the array is dominated by fluxon avalanches as is shown in the Fig.1b where arrows indicate approximately the start of a series of sharp increases in rotation number, this mechanism is referred as "avalanches or burst regime". For higher (subcritical) current values avalanches become less evident because the array almost continuosly is penetrated by a large number of fluxons, so we refers to this as "continuos flux diffusion regime" (cf. Fig.1a).

Fig.1a

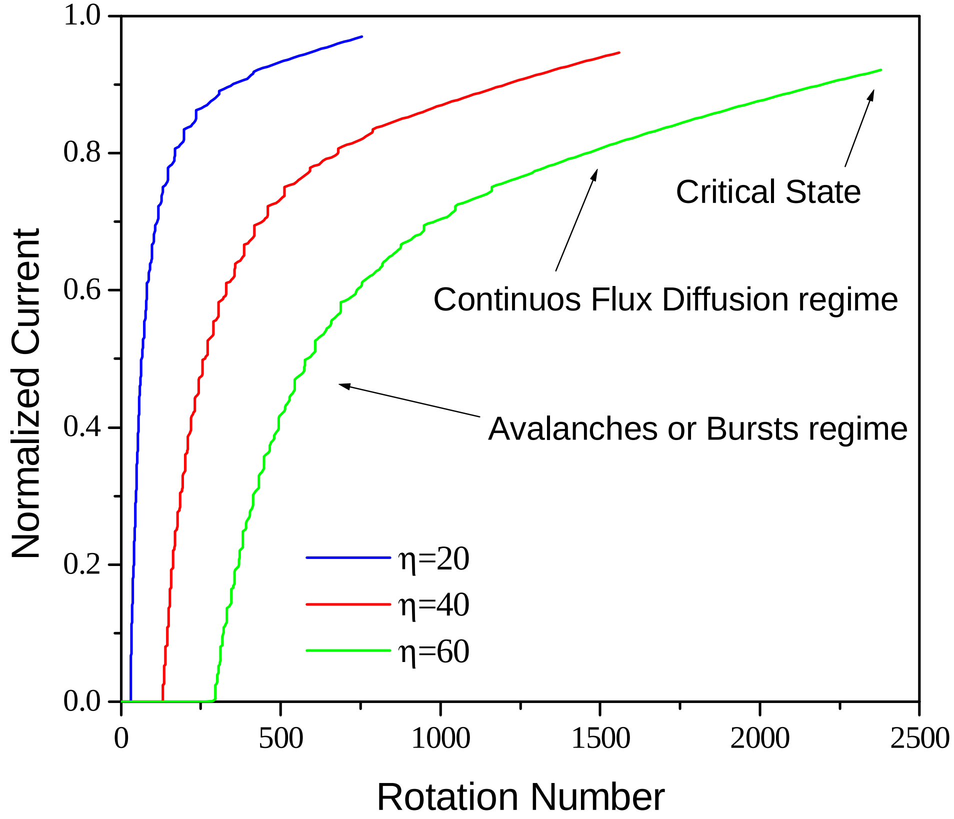
1.0
0.8
0.6
0.4
0.2
0.0
0
500
1000
1500
2000
2500
Normalized Current
Rotation Number
Critical State
Continuos Flux Diffusion regime
Avalanches or Bursts regime
η=20
η=40
η=60

Fig.1b

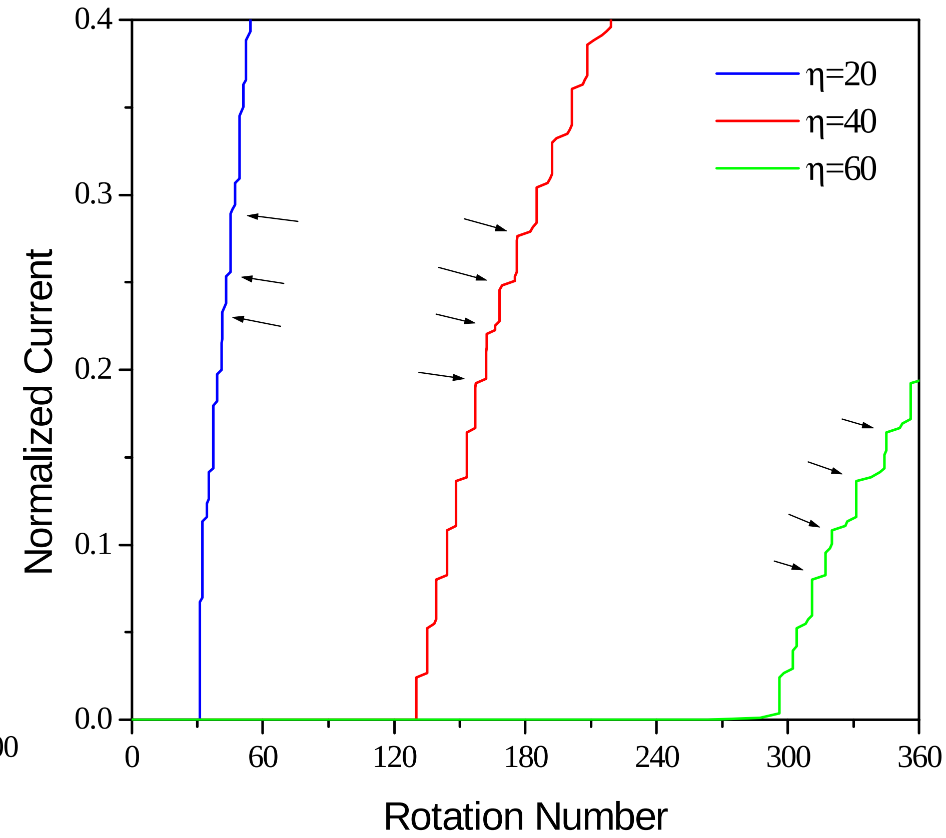
0.4
0.3
0.2
0.1
0.0
0
60
120
180
240
300
360
Normalized Current
Rotation Number
η=20
η=40
η=60

In Fig.2 is shown the normalized magnetic flux distribution $h=\Delta\varphi/2\pi$, evalued as phase difference $\Delta\varphi=\varphi_{k+1}-\varphi_k$, over the array, i.e., the number of flux quanta for each cell in the array. In Fig.2a for a given value of external normalized magnetic field the number of flux quanta in each cell is shown for different values of current. Higher currents corresponds to complete penetration of flux in the array, whereas lower current the flux is essentially concentrated near the active end. The flux distribution is essentially linear (Bean) and also for higher subcritical currents is clear that passive end is again untouched by flux penetration occurring also at few cells of distance, thus confirming that criticality is connected to full penetration. In Fig.2b the magnetic flux distribution is plotted just before and after the process of penetration of an avalanche of fluxons in the array in the "avalanche regime", can be view how fluxon will distribute along the first cells near active end. The parameters of the array are the following: $\beta_L=225$, $N=40$, $\alpha=1$, the normalized magnetic field is $\eta=40$.

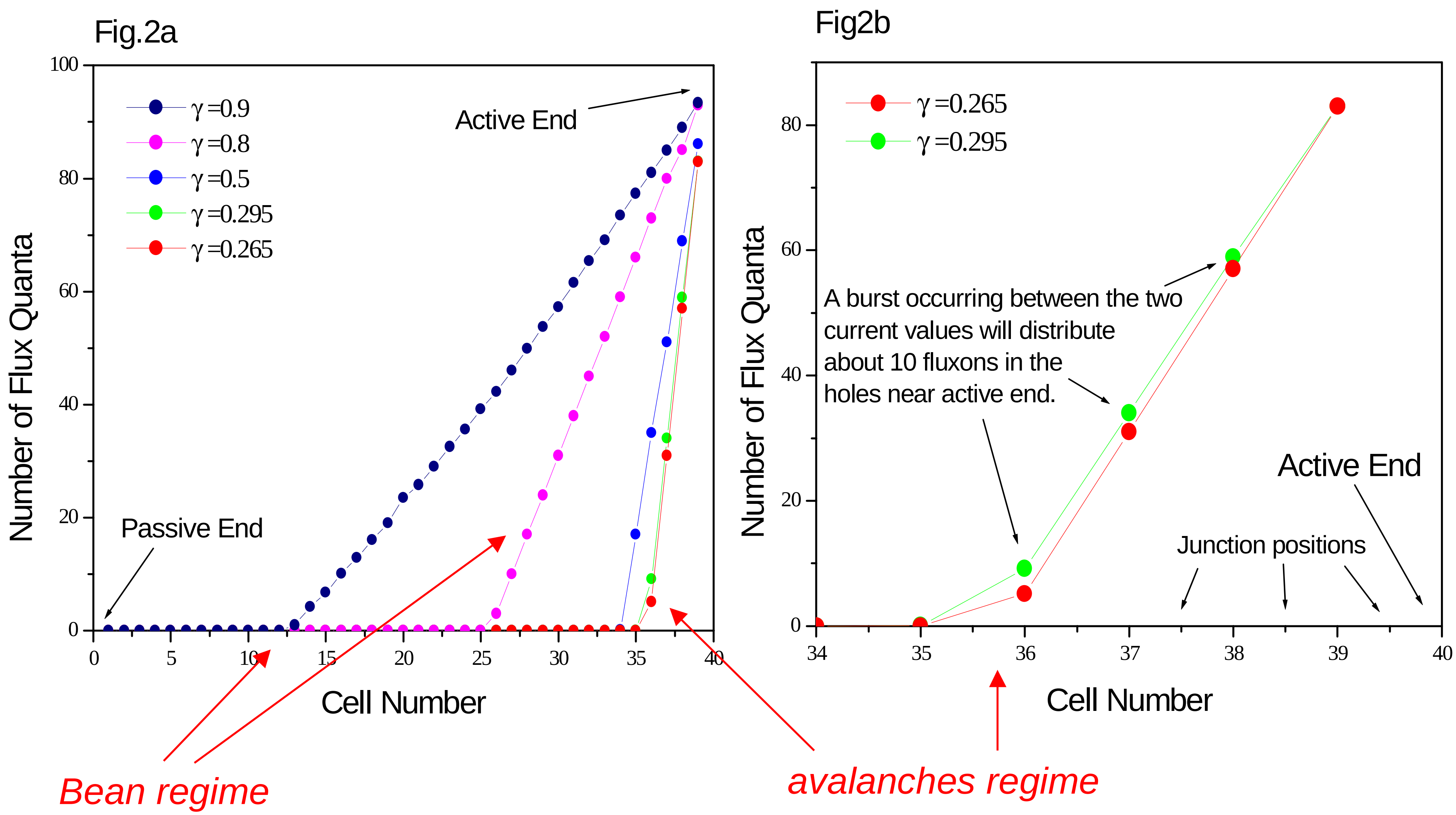

Fig.2a
Number of Flux Quanta
Cell Number
γ=0.9
γ=0.8
γ=0.5
γ=0.295
γ=0.265
Active End
Passive End
Bean regime
avalanches regime
Fig2b
γ=0.265
γ=0.295
A burst occurring between the two current values will distribute about 10 fluxons in the holes near active end.
Active End
Junction positions

We show that the plateau like shape of the J_c vs B curve can be reproduced also in this case. In Fig.3a we show the magnetic field pattern for a small array of N=10 JJ. The plateau extends over some decades like in the experimental data, values of β_L can be as high as 6400 to obtain the longest plateau. In Fig.3b the same plateau is shown for an array of N=40 JJ. The plateau extends approximately over the same length of previous case, but values of β_L are relatively smaller, ranging from 25 to 400. So the plateau length depends on the coupling β_L between the JJ and the number of JJ in the array. It is found that the normalized crossover field b* depends roughly on $N\beta_L^{1/2}$ in all simulations, so also for small values of β_L (typically between 1 and 10) should be possible have *large* value of b* if the number of junctions is high (however for such small β_L effects of mutual inductance cannot be typically ignored and a full inductance model have to be considered). In all simulations α=1.

Fig.3a

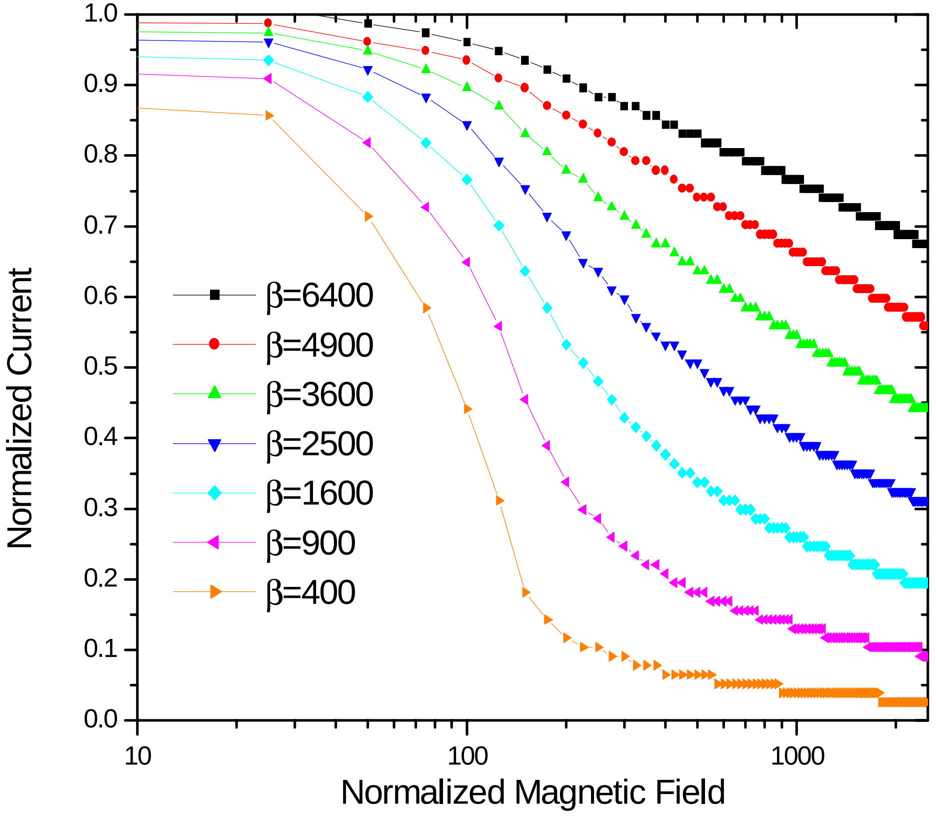

N = 10 JJ

Fig.3b

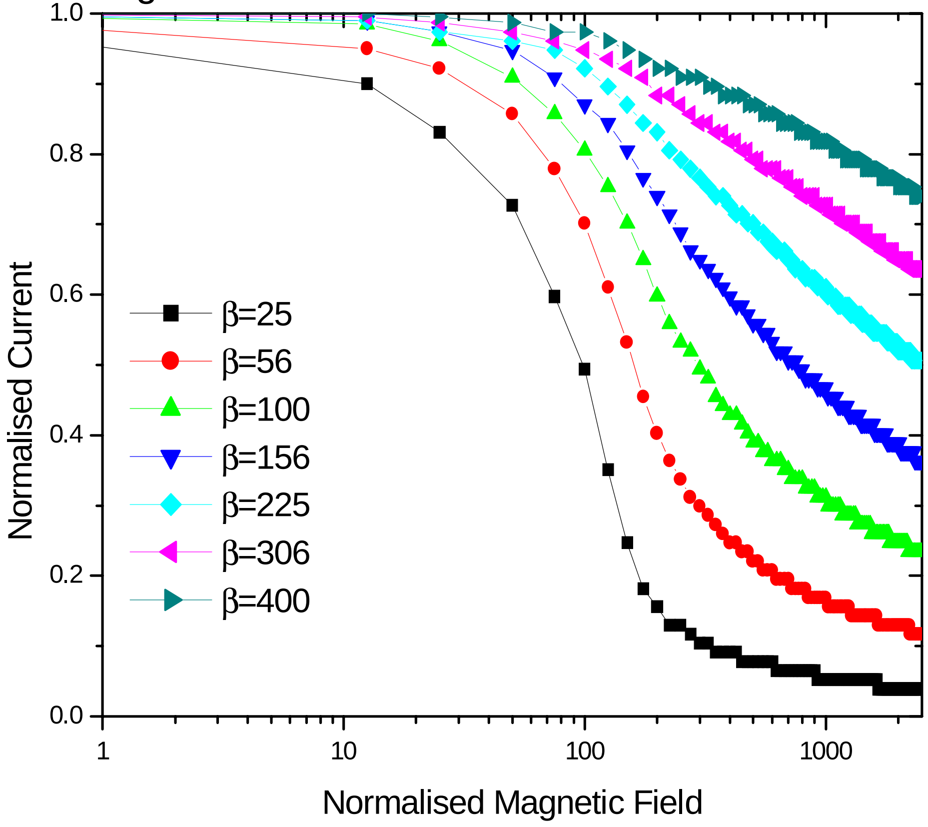

N = 40 JJ

The experimental dependence of the critical current density on the applied magnetic field in YBCO thin films has been obtained from susceptibility measurements [2]. Fig.4a and Fig.4b show typical results for different temperatures and for films with different oxygen content.
The characteristic feature is the plateau in the J_c vs. log B curves, that can be explained in terms of Josephson currents through the nanosized granular structure of the film [2].
It has been shown that such links have a statistical length distribution, with a mean value of the order of 20 nm [5].

Fig.4a

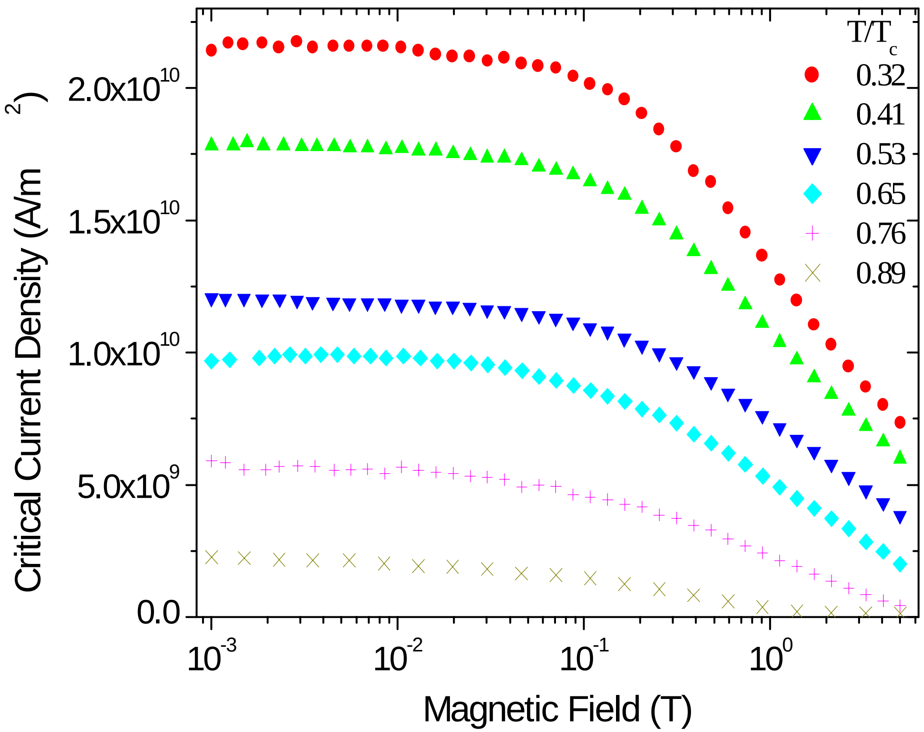

T/T$_c$
0.32
0.41
0.53
0.65
0.76
0.89
Critical Current Density (A/m^2)
2.0x10^{10}
1.5x10^{10}
1.0x10^{10}
5.0x10^{9}
0.0
10^{-3}
10^{-2}
10^{-1}
10^{0}
Magnetic Field (T)

Fig.4b

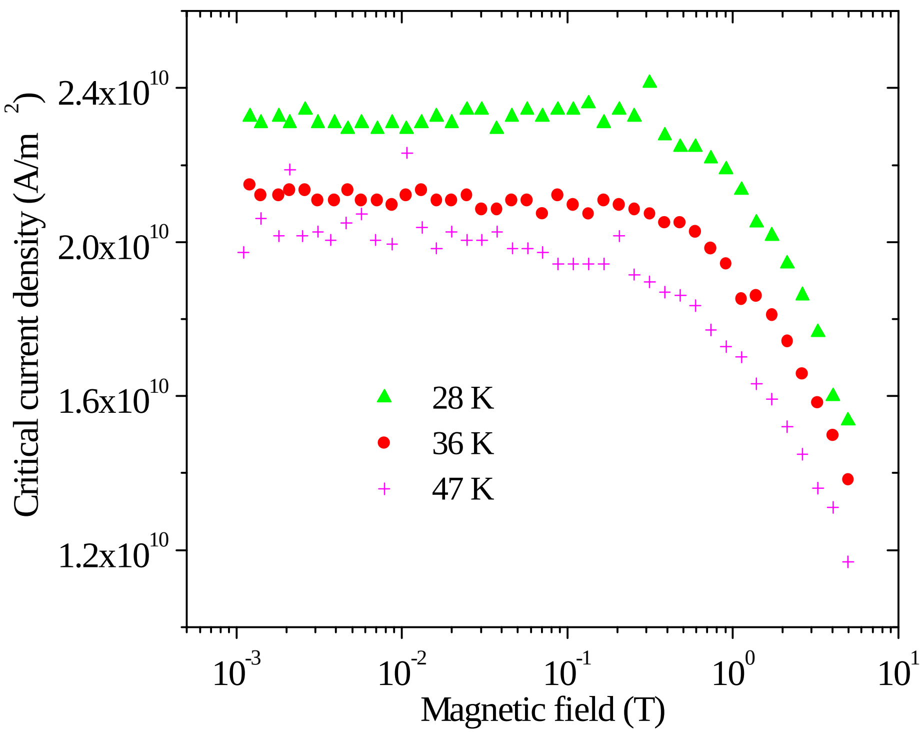

Critical current density (A/m^2)
2.4x10^{10}
2.0x10^{10}
1.6x10^{10}
1.2x10^{10}
28 K
36 K
47 K
10^{-3}
10^{-2}
10^{-1}
10^{0}
10^{1}
Magnetic field (T)

Part II - Conclusions

In this model all junctions in the array are supposed identical (same critical current and dissipation) and pointlike JJ and moreover cells in the array are supposed have similar inductances which is obviously not the case for the true superconducting HTC films. We note that a spread in the junction parameters via statistical distribution of parameters can add some quantitavive difference in the set up of critical state, because pinning barriers will vary within the array so giving arise to more disordered flux distribution, but we expect no qualitative substantial differences in the global behavior of the array especially in the plateau feature. Most important here, also for the comparison with experimental data (cf. Fig.4), is the fact that junctions are typically not pointlike object but can shown a distribution of lengths on nanometric scale. This implies that JJ in the array cannot be treated in principle as pointlike object, though they have to be considered short junctions. Further investigations on these points are in progress.

Acknowledgment

This work was supported on MURST COFIN98 Project “Dinamics and Thermodynamics of vortex structures in superconductive tunneling".

References

1. F. Parodi and R.Vaccarone, Physica **C173**, 56-64, 1991.
2. E. Mezzetti et al, Phys. Rev. **B60**, 7623, 1999.
3. C. Lucheroni, Phys.Rev.**B55**, 6559, 1997.
4. G. Filatrella, A. Petraglia and G. Rotoli, Eur.J.Phys. **12**, 23-30, 1999.
5. E. Mezzetti et al., Physica **C332**, 126, 2000.

This publication is based (partly) on the presentations made at the European Research Conference (EURESCO) on "Future Perspectives of Superconducting Josephson Devices: Euroconference on Physics and Application of Multi-Junction Superconducting Josephson Devices, Acquafredda di Maratea, Italy, 1-6 July 2000, organised by the European Science Foundation and supported by the European Commission, Research DG, Human Potential Programme, High-Level Scientific Conferences, Contract HPCFCT-1999-00135. This information is the sole responsibility of the author(s) and does not reflect the ESF or Community's opinion. The ESF and the Community are not responsible for any use that might be made of data appearing in this publication."